VIP Organic Semiconductors

DOI: 10.1002/ange.201302396

Doping of Organic Semiconductors: Impact of Dopant Strength and Electronic Coupling**

Henry Méndez, Georg Heimel, Andreas Opitz, Katrein Sauer, Patrick Barkowski, Martin Oehzelt, Junshi Soeda, Toshihiro Okamoto, Jun Takeya, Jean-Baptiste Arlin, Jean-Yves Balandier, Yves Geerts, Norbert Koch, and Ingo Salzmann**

Doping inorganic semiconductors is key for device functionality. It allows the precise adjustment of the position of the Fermi level relative to the semiconductor transport levels, thus also controlling energy barriers for charge injection. Furthermore, it reduces ohmic losses in transport layers through increased conductivity, even at minimal doping levels. In the rapidly growing field of organic electronics, where organic semiconductors (OSCs) are the active component, analogous doping-related benefits are aspired in order to realize devices that operate on the basis of the same well-proven principles and, ideally, display comparable performance. However, despite the emergence of the entire field through the discovery of a doping-induced conductivity increase in polymeric[1] and small-molecule OSCs[2] by up to 11 orders of magnitude, most of today's devices are still based on intrinsic materials, as doping with alkali metals or halides turned out to be problematic due to their reactivity and tendency to diffuse.[3]

Recent benchmark organic electronic devices have demonstrated that these problems can, to a large part, be eliminated by resorting to molecular electrical doping instead.[4,5] There, stable p[n]-type doping is realized by admixing strong molecular acceptors [donors] to OSC films with the electron affinity (EA) [ionization energy (IE)] of the dopant molecule in the range of the IE [EA] of the OSC. Interestingly, however, compared to inorganic semiconductor doping as well as alkali metal/halide doping, significantly lower doping efficiencies are reached by this approach, the reasons for which are still under debate.[5,6]

Also the microscopic mechanism of molecular electrical doping faces some controversy at present. The "standard" model is based on concepts adopted from inorganic semiconductor physics. Integer charge transfer from the highest occupied molecular orbital (HOMO) of the OSC to the lowest unoccupied molecular orbital (LUMO) of the p-dopant, and vice versa for n-type doping, is assumed. This mutual ionization is then argued to result in a localized charge on the dopant and a mobile hole [electron] in the OSC matrix, in other words, positive [negative] polarons for p[n]-type doping, as illustrated in Figure 1a for p-type doping.[5,7–12] This model requires the EA of a powerful p-type dopant to be as high as possible, and this has stimulated considerable research efforts in the design and synthesis of such materials.[5,13,14] Although most are still less efficient than anticipated, further increasing the acceptor EA is expected to eventually lead to complete mutual ionization of OSC and p-dopant.

Recently, an alternative model for the fundamental process of molecular electrical doping has been proposed.[15–18] For the prototypical OSC/p-dopant pair pentacene and 2,3,5,6-tetrafluoro-7,7,8,8-tetracyanoquinodimethane (**2d** in Figure 1d), frontier molecular orbital hybridization between the OSC HOMO and the dopant LUMO has been suggested, leading to the formation of a ground-state charge-transfer complex with a reduced energy gap between a doubly occupied bonding and an unoccupied antibonding hybrid orbital (Figure 1b). For p-type doping, the latter lies within the fundamental gap of the OSC (Figure 1c), as the former does for n-type doping. Occupation of all available states following Fermi–Dirac statistics then readily explains the comparably low doping efficiency, as only a fraction of the complexes is ionized at room temperature.[15,16] Additionally, frontier molecular orbital hybridization contributes to a substantial intermolecular binding energy, which acts as a driving

[*] H. Méndez, G. Heimel, A. Opitz, K. Sauer, P. Barkowski, M. Oehzelt, N. Koch, I. Salzmann
Humboldt-Universität zu Berlin, Institut für Physik
Brook-Taylor-Strasse 6, 12489 Berlin (Germany)
E-mail: georg.heimel@physik.hu-berlin.de
ingo.salzmann@physik.hu-berlin.de
M. Oehzelt, N. Koch
Helmholtz Zentrum Berlin für Materialien und Energie – BESSY II
Albert-Einstein-Strasse 15, 12489 Berlin (Germany)
J. Soeda, T. Okamoto, J. Takeya
Osaka University, Institute of Scientific and Industrial Research (ISIR)
Mihogaoka 8–1, Ibaraki, Osaka, 567-0047 (Japan)
J.-B. Arlin, J.-Y. Balandier, Y. Geerts
Université Libre de Bruxelles (ULB), Chimie des Polymères
CP206/1 Boulevard du Triomphe, 1050 Bruxelles (Belgium)
H. Méndez
Pontificia Universidad Javeriana, Departamento de Física
Carrera 7 No. 43-82 Ed.52, Bogotá (Colombia)

[**] We thank Paul Zybarth and Timo Florian (HU Berlin), Wolfgang Caliebe (DESY—HASYLAB), and Roland Resel and Alexander Pichler (TU Graz, Austria) for experimental support, Günter Wagner (Leibniz Institut für Kristallzüchtung) for film-thickness measurements, and Armin Moser (TU Graz, Austria) for providing the software package PyGid. This research was financially supported by the Academic Vice-Rectorate of Pontificia Universidad Javeriana (Colombia) and the Katholischer Akademischer Ausländer Dienst (KAAD) (H.M.), as well as by the ARC program of the Communauté française de Belgique (grant no. 20061 to Y.G., J.Y.B., J.B.A.).

Supporting information for this article is available on the WWW under http://dx.doi.org/10.1002/anie.201302396.

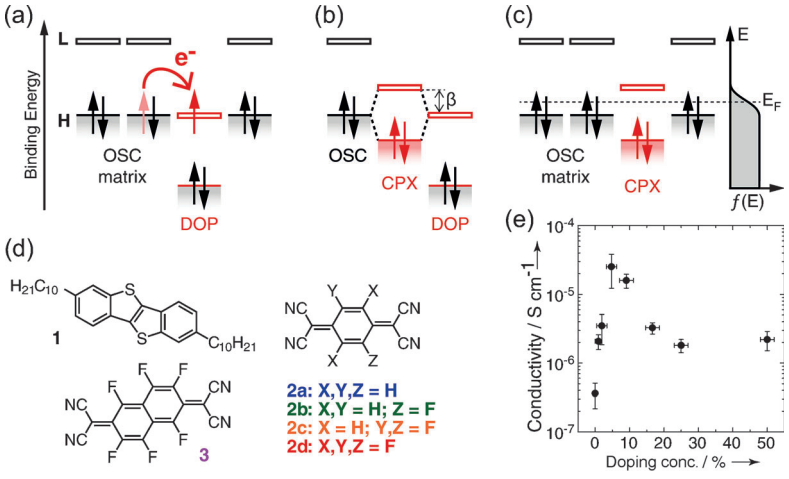

Figure 1. a) Standard model for molecular electrical doping assuming integer charge transfer from the HOMO (H) of the OSC to the LUMO (L) of the p-dopant (DOP) leading to ionized molecules. b) Alternative model assuming the hybridization of the frontier molecular orbitals of the OSC and the p-dopant in a supramolecular complex (CPX); β denotes the resonance integral. c) Complexes within the OSC matrix exhibit low-lying unoccupied states in the OSC gap, which are occupied according to Fermi–Dirac distribution [*f*(E)]; shaded/white boxes denote HOMO/LUMO levels. d) Chemical structures of **1**, **2a–d**, and **3**. e) Conductivity of films of **1** with increasing amount of dopant **2d**.

constant and known, as should the nodal structure of the respective frontier molecular orbitals. We chose to combine 2,7-didecyl[1]benzothieno-[3,2-b][1]benzothiophene (**1**) as OSC[21–23] with tetracyanoquinodimethane (**2a**) and its fluorinated derivatives **2b**, **2c**, and **2d** as p-dopants (Figure 1d).[7,24] Alkylated benzothienobenzothiophene has been already employed as OSC in high-mobility field effect transistors[21–23] and **2a–d** are prototypical p-dopants that feature a systematic increase in EA upon increasing degree of fluorination (from 4.23–5.08 eV[24]) with only minor changes to their LUMO wavefunctions (see the Supporting Information). Our study is complemented by the recently introduced strong p-dopant 2,2′-(perfluoronaphthalene-2,6-diylidene)dimalononitrile (**3**; see Figure 1d).[25–27]

That the OSC **1** can be effectively p-doped with molecular acceptors is shown exemplarily for **2d** in Figure 1e. Upon dopant admixture, we observe an increase in conductivity by two orders of magnitude, which decreases again beyond a dopant concentration of 5%. This behavior is typical for molecular electrical

force for complex formation. The magnitude of this energy-level splitting, which, in a Hückel-like picture, is captured by an intermolecular resonance integral β (sometimes also referred to as transfer integral *t*),[19] is not only determined by the individual OSC and dopant energy levels, but also by the nodal structure of their frontier orbitals and, finally, by their relative orientation.[20] In contrast to the standard model, the doping efficiency is limited by β in this perception, as finite (and potentially substantial) frontier molecular orbital splitting is retained in the complex even upon increasing the dopant EA (see Figure 1b for IE = EA).

Here, we aim at testing which strategy is more promising for enhancing the efficiency of molecular dopants in small-molecule OSCs: increasing the dopant EA, as emerging from the standard model, or reducing β, as the model of complex formation suggests. To this end, material combinations are required such that the dopant EA can be varied without changing β; that is, the relative orientation of OSC and dopant should be both

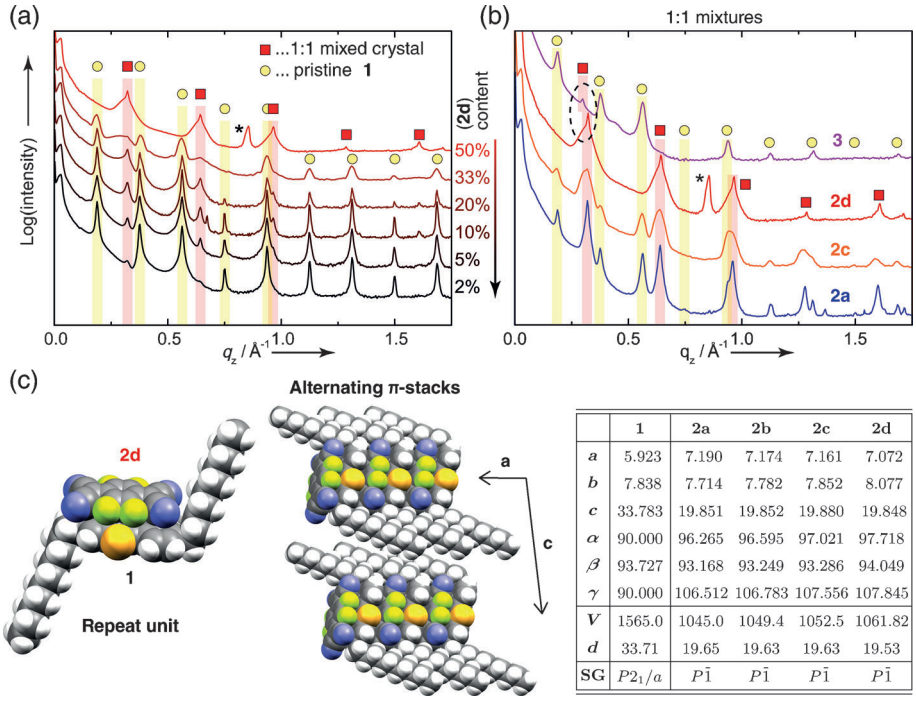

	1	2a	2b	2c	2d
a	5.923	7.190	7.174	7.161	7.072
b	7.838	7.714	7.782	7.852	8.077
c	33.783	19.851	19.852	19.880	19.848
α	90.000	96.265	96.595	97.021	97.718
β	93.727	93.168	93.249	93.286	94.049
γ	90.000	106.512	106.783	107.556	107.845
V	1565.0	1045.0	1049.4	1052.5	1061.82
d	33.71	19.65	19.63	19.63	19.53
SG	$P2_1/a$	$P\bar{1}$	$P\bar{1}$	$P\bar{1}$	$P\bar{1}$

Figure 2. a) Specular XRD on films of **1** doped with **2d** at different ratios. Yellow circles mark the peak series of pure OSC **1**,[23] red squares that of 1:1 cocrystals; the asterisk marks a contribution of excess **2d**.[35] b) Specular XRD on 1:1 mixed films of **1** with **2a**, **c**, **d** shows growth of essentially identical mixed crystal structures (red squares) while that with **3** has an increased out-of-plane lattice spacing (marked with a dashed oval). c) Left: Repeat unit of the mixed crystal structures shown for **2a**. Left: View along the *b*-axis illustrating the alternating π-stacks in the *a*-direction and the out-of-plane lattice spacing in the *c*-direction. Right: Unit-cell parameters of **1**[23] and its mixed crystals with acceptors **2a–d** determined by single-crystal diffraction; *a*, *b*, *c* in Å; α, β, γ in degrees; *d* values are the respective d_{001} lattice spacings (in Å); *V* denotes the unit-cell volumes and SG the respective space group.

doping;[7–12,15,28,29] the steep initial increase in conductivity at low concentrations has been attributed to trap filling.[30,27]

To ascertain that the molecular packing in our systems indeed remains constant when the dopant EA is varied, we carried out specular X-ray diffraction (XRD) experiments on drop-cast films of **1** doped with **2d** on SiO_x substrates and found two series of peaks. The first (yellow circles in Figure 2a) is readily assigned to pure **1** on the basis of its known single-crystal structure.[23] In view of the equally crystalline nature of the 1:1 mixed film and the absence of signal from pure **1**, the assignment of the second series of peaks (red squares) to a 1:1 mixed crystal structure emerges naturally. Its persistence down to application-relevant dopant concentrations of 2% without significant changes to the characteristic lattice spacings indicates that it is indeed the presence of this structure, and the intermolecular electronic coupling therein, which is responsible for doping (see Figure 1e).

Almost identical growth of mixed crystals is observed in 1:1 films with **2a–c** as shown in Figure 2b; only the out-of plane lattice spacing for **3** is slightly increased owing to its different molecular shape (see Figure 1d). To determine the relative molecular orientation within the 1:1 mixed phases, we solved the structures of single crystals grown from equimolar solutions of **1** and **2a–d** in chloroform (see the table in Figure 2c and the Supporting Information for CIF files). As shown for **2d** in Figure 2c, the basic repeat unit consists of the acceptor interacting with the π-conjugated core of **1**. Repetition of this motif along the *a*-direction of the unit cell results in alternating π-stacks. The lattice spacing in the *c*-direction allowed assigning the peak series of the 1:1 mixed films in Figure 2a,b to the respective (00ℓ) reflections. Performing, in addition, grazing-incidence XRD reciprocal-space mapping confirms that single crystals and thin films are fully isostructural for all dopants (see the Supporting Information). Overall, XRD studies indicate that the relative orientation between **1** and **2a–d** is virtually constant upon tuning EA. The potential impact of changes in molecular packing on the energy levels in the mixed films is thus minimized, which ensures that the resonance integral β between OSC HOMO and dopant LUMO varies little among all investigated compounds.

Having established structural comparability of our samples, we turn to the consequences of varying the dopant EA on their electronic structure as inferred from optical absorption (UV/Vis) spectroscopy. Spectra of films of **1** with different **2d** content are shown in Figure 3a in comparison to the spectra of the respective pure materials. Pristine **1** (black curve) exhibits its fundamental transition at 3.42 eV (peak) while the optical gap of **2d** is at 2.6 eV (gray curve). Admixture of **2d** to **1** gives rise to new transitions (labeled T1 and T2) at energies lower than the fundamental absorptions of the pure materials; these transitions increase in intensity with the doping ratio until they dominate the spectrum of the 1:1 mixed film. We note that typical doping levels in devices are in the single-digit percentage range, where the sensitivity of our experiment would be too low to clearly observe these transitions (Figure 3a). However, in the systems considered here, their intensity can be "amplified"

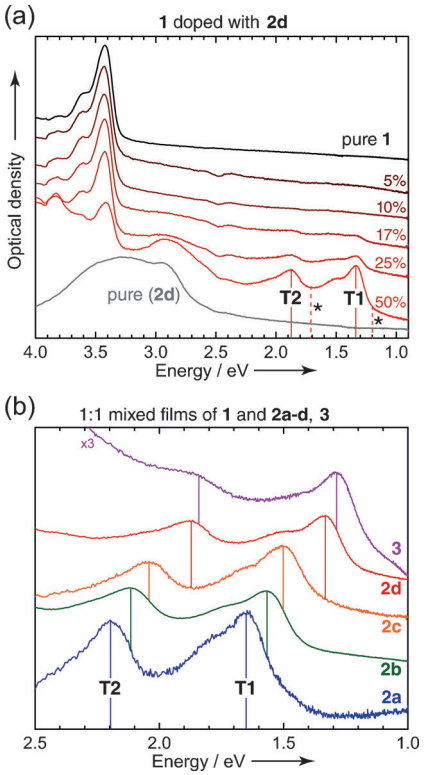

Figure 3. a) UV/Vis absorption spectra of films of **1** doped with **2d** at different ratios and of pure **1** (black curve) and pure **2d** (gray curve); the two lowest-energy transitions (T1 and T2) are assigned to the complex and indicated with solid vertical lines; respective transitions calculated by TDDFT are marked with dotted lines and stars. b) Spectra of 1:1 mixed films for all investigated dopants (for full spectra and lower doping concentrations see the Supporting Information). All spectra are measured down to 0.6 eV, no further transitions are observed; films were spin-coated from chloroform solution on quartz substrates.

without altering their origin: Irrespective of concentration, T1 and T2 represent the spectral signature of a single well-defined species, that is, complexes of acceptor **2d** and OSC **1** with their respective π-systems in close contact, as established by XRD. Analogous results obtained for 1:1 mixed films with **2a–c** and **3** as p-dopants are illustrated in Figure 3b; for other mixing ratios and full spectra see the Supporting Information.

Notably, the energies of T1 and T2 decrease with increasing dopant EA, while their energy spacing stays essentially constant. According to the standard model of molecular electrical doping, transitions related to the ionized species of both **2a–d** and **1** would be expected, with that of the OSC remaining at a fixed energy upon dopant variation. This is, however, not the case (Figure 3b). Furthermore, T1 and T2 do not correspond to the optical transitions of the ionized dopants (see the Supporting information).[31–34] Both observations disagree with the notion of mutual ionization. We note on the side that, as evident from the diagram in Figure 4, T1 and T2 cannot stem from charge-transfer excitations between the HOMO of **1** and the LUMO of the dopants either, because the lower-energy T1 is always higher in energy

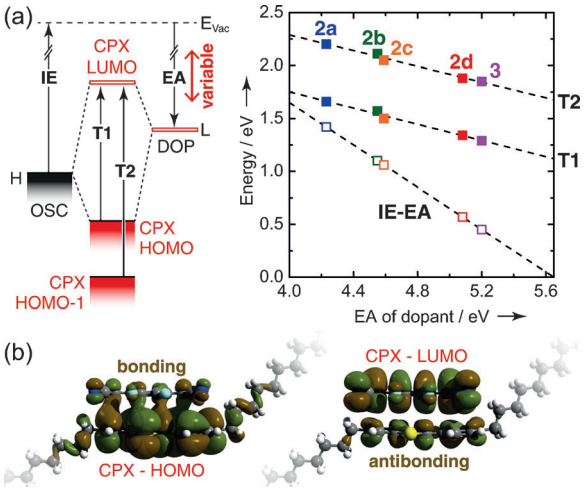

Figure 4. a) Left: Schematic energy level diagram of OSC, p-dopants (DOP) of variable EA, and the supramolecular complex (CPX). T1 and T2 denote transitions between the HOMO and the HOMO-1 of the complex to its LUMO. Right: Experimental values of T1 and T2 taken from Figure 3b (filled squares) for all dopants and the respective difference between the IE of **1** [= 5.65 eV, as calculated by DFT, see the Supporting Information] and the EA of the respective dopant (open squares) are plotted against EA. EA values for **2a–d** taken from Ref. [24]; that for **3** is calculated by DFT, see the Supporting Information. b) Orbital isosurface plots of the supramolecular hybrid orbitals calculated for an isolated complex of **1** and **2d** by DFT.

than the energy difference between the respective frontier molecular orbitals.

If, in contrast, one assumes the formation of a charge-transfer complex between **1** and **2a–d,** or **3**, T1 and T2 can readily be assigned to the HOMO/LUMO and HOMO-1/LUMO transitions of the complex on the basis of time-dependent density functional theory (TDDFT) calculations for isolated complexes of all investigated OSC/dopant pairs (calculated transition energies indicated by dashed vertical lines in Figure 3a). As shown in Figure 4, a linear fit to the transition energies yields a value of roughly 1.18 eV for T1 in the (hypothetical) case of the dopant EA being equal to the IE of **1**. Importantly, this illustrates that even if the IE of the OSC and the EA of the dopant were perfectly matched, a substantial energy-level splitting would remain and severely limit the efficiency of molecular electrical doping (cf. Figure 1b). From the known frontier orbital energies of pure OSC and pure dopants (HOMO and LUMO, respectively) as well as from the measured energies of the T1 transitions, very similar values for β (in the range of 0.4–0.6 eV) are extracted from a simple Hückel-like treatment. Conversely, assuming a constant value of $\beta = 0.55$ eV reproduces the dependence of T1 on the (see the Supporting Information for details).

With these results we can now compare the standard model for molecular electrical doping (assuming integer charge transfer between OSC and dopant) to the alternative model based on the formation of a charge-transfer complex in terms of the applicability of the respectively emerging design strategies for improved molecular dopants: In addition to the general prerequisite of the OSC IE being in the range of the dopant EA, which is still valid in the model based on complex formation, β needs to be minimized in order to reduce the energy-level splitting in the complex. Lowering this splitting directly translates into lowering the energy of the unoccupied hybrid states in the OSC gap (cf. Figure 1c) and, thus, into higher doping efficiencies by increasing the number of ionized complexes at room temperature. Our observations highlight that the design strategy emerging from the standard model, that is, increasing the p-dopant EA, is not sufficient. Its single demand should be supplemented by the additional criterion emerging from the alternative model, that is, reducing the intermolecular resonance integral β. Preventing the dopant frontier molecular orbitals from overlapping with those of the OSC by steric shielding therefore emerges as promising strategy for the chemical design of improved dopants.

Received: March 21, 2013
Published online: June 19, 2013

Keywords: doping · electronic structure · semiconductors · UV/Vis spectroscopy

[1] H. Shirakawa, E. J. Louis, A. G. Macdiarmid, C. K. Chiang, A. J. Heeger, *J. Chem. Soc. Chem. Commun.* **1977**, 578–580.
[2] Y. Yamamoto, K. Yoshino, Y. Inuishi, *J. Phys. Soc. Jpn.* **1979**, *47*, 1887–1891.
[3] G. Parthasarathy, C. Shen, A. Kahn, S. R. Forrest, *J. Appl. Phys.* **2001**, *89*, 4986–4992.
[4] S. Reineke, F. Lindner, G. Schwartz, N. Seidler, K. Walzer, B. Lüssem, K. Leo, *Nature* **2009**, *459*, 234–238.
[5] B. Lüssem, M. Riede, K. Leo, *Phys. Status Solidi A* **2013**, *210*, 9–43.
[6] P. Pingel, R. Schwarzl, D. Neher, *Appl. Phys. Lett.* **2012**, *100*, 143303.
[7] K. Walzer, B. Maennig, M. Pfeiffer, K. Leo, *Chem. Rev.* **2007**, *107*, 1233–1271.
[8] "Controlled doping of molecular organic layers: Physics and device prospects" in M. Pfeiffer, T. Fritz, J. Blochwitz, A. Nollau, B. Plönnigs, A. Beyer, K. Leo, *Advances in Solid State Physics*, *Vol. 39*, Springer, Berlin, **1999**, 77–90.
[9] W. Y. Gao, A. Kahn, *J. Phys. Condens. Matter* **2003**, *15*, S2757–S2770.
[10] W. Y. Gao, A. Kahn, *J. Appl. Phys.* **2003**, *94*, 359–366.
[11] W. Y. Gao, A. Kahn, *Appl. Phys. Lett.* **2001**, *79*, 4040–4042.
[12] K. Harada, M. Riede, K. Leo, O. R. Hild, C. M. Elliott, *Phys. Rev. B* **2008**, *77*, 195212.
[13] Y. B. Qi, T. Sajoto, S. Barlow, E. G. Kim, J. L. Brédas, S. R. Marder, A. Kahn, *J. Am. Chem. Soc.* **2009**, *131*, 12530.
[14] R. Meerheim, S. Olthof, M. Hermenau, S. Scholz, A. Petrich, N. Tessler, O. Solomeshch, B. Lüssem, M. Riede, K. Leo, *J. Appl. Phys.* **2011**, *109*, 103102.
[15] I. Salzmann, G. Heimel, S. Duhm, M. Oehzelt, P. Pingel, B. M. George, A. Schnegg, K. Lips, R. P. Blum, A. Vollmer, N. Koch, *Phys. Rev. Lett.* **2012**, *108*, 035502–035507.
[16] G. Heimel, I. Salzmann, N. Koch, *AIP Conf. Proc.* **2012**, *1456*, 148–156.
[17] E. E. Aziz, A. Vollmer, S. Eisebitt, W. Eberhardt, P. Pingel, D. Neher, N. Koch, *Adv. Mater.* **2007**, *19*, 3257–3260.
[18] P. Pingel, L. Y. Zhu, K. S. Park, J. O. Vogel, S. Janietz, E. G. Kim, J. P. Rabe, J. L. Brédas, N. Koch, *J. Phys. Chem. Lett.* **2010**, *1*, 2037–2041.
[19] V. Coropceanu, J. Cornil, D. A. da Silva Filho, Y. Olivier, R. Silbey, J. L. Brédas, *Chem. Rev.* **2007**, *107*, 926–952.

[20] Note that the packing was undefined in the study on pentacene/**2a** as, there, the mixed films turned out to be amorphous at higher doping ratios.[25,15]
[21] H. Ebata, T. Izawa, E. Miyazaki, K. Takimiya, M. Ikeda, H. Kuwabara, T. Yui, *J. Am. Chem. Soc.* **2007**, *129*, 15732.
[22] T. Uemura, Y. Hirose, M. Uno, K. Takimiya, J. Takeya, *Appl. Phys. Express* **2009**, *2*, 111501.
[23] T. Izawa, E. Miyazaki, K. Takimiya, *Adv. Mater.* **2008**, *20*, 3388.
[24] K. Kanai, K. Akaike, K. Koyasu, K. Sakai, T. Nishi, Y. Kamizuru, T. Nishi, Y. Ouchi, K. Seki, *Appl. Phys. A* **2009**, *95*, 309 – 313.
[25] H. Kleemann, C. Schuenemann, A. A. Zakhidov, M. Riede, B. Lüssem, K. Leo, *Org. Electron.* **2012**, *13*, 58 – 65.
[26] C. Weichsel, L. Burtone, S. Reineke, S. I. Hintschich, M. C. Gather, K. Leo, B. Lüssem, *Phys. Rev. B* **2012**, *86*, 075204.
[27] M. L. Tietze, L. Burtone, M. Riede, B. Lüssem, K. Leo, *Phys. Rev. B* **2012**, *86*, 035320.
[28] S. D. Ha, A. Kahn, *Phys. Rev. B* **2009**, *80*, 195410.
[29] K. Harada, M. Sumino, C. Adachi, S. Tanaka, K. Miyazaki, *Appl. Phys. Lett.* **2010**, *96*, 253304.
[30] S. Olthof, S. Mehraeen, S. K. Mohapatra, S. Barlow, V. Coropceanu, J. L. Brédas, S. R. Marder, A. Kahn, *Phys. Rev. Lett.* **2012**, *109*, 176601.
[31] L. R. Melby, R. J. Harder, W. R. Hertler, W. Mahler, R. E. Benson, W. E. Mochel, *J. Am. Chem. Soc.* **1962**, *84*, 3374 – 3387.
[32] I. Zanon, C. Pecile, *J. Phys. Chem.* **1983**, *87*, 3657 – 3664.
[33] T. Shimizu, T. Yamamoto, *Inorg. Chim. Acta* **1999**, *296*, 278 – 280.
[34] D. T. Duong, C. Wang, E. Antono, M. F. Toney, A. Salleo, *Org. Electron.* **2013**, *14*, 1330 – 1336.
[35] T. J. Emge, M. Maxfield, D. O. Cowan, T. J. Kistenmacher, *Mol. Cryst. Liq. Cryst.* **1981**, *65*, 161 – 178.

